

DISSIPATION-BASED APPROACH AND ROBUST INTEGRATION ALGORITHM FOR 3D PHENOMENOLOGICAL CONSTITUTIVE MODELS FOR SHAPE MEMORY ALLOYS

Edoardo Artioli and Paolo Bisegna

Department of Civil Engineering and Computer Science
University of Rome - Tor Vergata
via del Politecnico 1, 00133 Rome, Italy
E-mail: {artioli,bisegna}@ing.uniroma2.it
URL: www.dicii.uniroma2.it

Key words: Shape Memory Alloy, Energetic Formulation, Dissipation, Singularity, Integration Algorithm.

Abstract. The paper presents an innovative dissipation-based solution algorithm for a phenomenological 3D constitutive model for shape memory alloys (SMA), set in the framework of generalized standard materials, within the formalism of thermodynamics of irreversible processes. The proposed solution scheme aims at detecting all mathematical singularities inherent to the formulation itself, and, in the discrete setting, is capable of filtering out the relevant numerical instabilities applying a check and treat paradigm. No regularization is introduced into the constitutive equations. Numerical results on single material point strain/stress - driven evolutions are reported to validate the proposed method.

1 INTRODUCTION

Thermodynamics with internal variables [1] is a well established framework for the development of constitutive models for shape memory alloys (SMA), consistent with the fundamental principles of thermodynamics. The main feature of this approach is to introduce an appropriate energy potential ψ (Helmholtz free energy) depending on *internal variables*, usually an inelastic macroscopic strain tensor \mathbf{e}^{tr} (*transformation strain*), and on observable control variables, usually a total strain tensor $\boldsymbol{\varepsilon}$ and the temperature T . Classically, constitutive equations are derived writing *state equations*, which define entities conjugate to the control variables and to the internal variables, together with a rate equation for the transformation strain. The latter is typically postulated as a flow rule associated to some plasticity-like yield function $f(\mathbf{X})$, or *transformation-function*, defining the elastic domain in terms of the stress measure \mathbf{X} , conjugate to \mathbf{e}^{tr} .

The present work focuses on the SMA constitutive model originally proposed by Souza et al. [2] and subsequently developed by Auricchio and Petrini [3], where a Helmholtz free energy function is considered, split into elastic, transformation, and chemical contributions. The energetic formulation of the constitutive model amounts to a nonlinear differential inclusion involving the total energy functional and the dissipation potential. This functional has non removable singularity points that need special treatment in regard to the solvability of the integrated constitutive equations. The proposed methodology filters out all the numerical instabilities connected to such singularities without any regularization of the model, and in particular provides the following results:

- A robust solution algorithm capable of checking admissibility of a solution either coinciding or falling in the nearness of a singularity point;
- An extension to a more general class of transformation functions, i.e. of dissipation mechanisms,
- A robust material model subroutine for FEM implementation.

Numerical tests on a single integration point are provided to prove such points.

2 SMA CONSTITUTIVE MODEL

The local thermodynamic state of the material is defined by the Green strain $\boldsymbol{\varepsilon}$, the absolute temperature T , regarded as control variables, and by the symmetric traceless¹ *transformation* strain tensor \mathbf{e}^{tr} describing the kinematics of the product phase. The Green strain is additively decomposed as:

$$\boldsymbol{\varepsilon} = \boldsymbol{\varepsilon}^e + \mathbf{e}^{\text{tr}} \quad (1)$$

being $\boldsymbol{\varepsilon}^e$ the elastic strain. The norm $\|\mathbf{e}^{\text{tr}}\|$ indicates a measure of the phase transition from the parent phase to the product phase, hence \mathbf{e}^{tr} is constrained to lie in the *saturation* domain $\mathcal{S} = \{\mathbf{e}^{\text{tr}} \in \text{SymDev} : \|\mathbf{e}^{\text{tr}}\| \leq \varepsilon_L\}$ [2]. The material parameter ε_L is related to the maximum transformation strain reached at the end of the forward isothermal transformation during a uniaxial test. Given its tensorial character, \mathbf{e}^{tr} is capable of representing the reorientation of the product phase in the saturated condition [4].

The Helmholtz free energy density ψ is assumed to be a strictly convex potential depending on the local state, given by:

$$\psi(\boldsymbol{\varepsilon}^e, \mathbf{e}^{\text{tr}}, T) = \psi^e(\boldsymbol{\varepsilon}^e) + \psi^{\text{ch}}(\mathbf{e}^{\text{tr}}, T) + \psi^{\text{tr}}(\mathbf{e}^{\text{tr}}) + \mathcal{I}_{\mathcal{S}}(\mathbf{e}^{\text{tr}}), \quad (2)$$

where:

¹In the following, the space of symmetric traceless second-order tensors is denoted by SymDev.

- ψ^e is the elastic strain energy, which, under the assumption of linear isotropic elasticity, is given by:

$$\psi^e(\boldsymbol{\varepsilon}^e) = \frac{1}{2}K(\text{tr } \boldsymbol{\varepsilon}^e)^2 + G\|\text{dev } \boldsymbol{\varepsilon}^e\|^2 \quad (3)$$

with K the bulk modulus and G the shear modulus;

- ψ^{ch} is the chemical energy, due to the thermally-induced martensitic transformation:

$$\psi^{\text{ch}}(\mathbf{e}^{\text{tr}}, T) = \beta\Delta T^+ \|\mathbf{e}^{\text{tr}}\| \quad (4)$$

with β a material parameter related to the dependence of the critical stress on the temperature, and $\Delta T^+ = \langle T - M_f \rangle$, being M_f the temperature corresponding to the end of the phase forward transformation, and $\langle \bullet \rangle$ the positive part of the argument;

- ψ^{tr} is the transformation strain energy, due to transformation strain hardening:

$$\psi^{\text{tr}}(\mathbf{e}^{\text{tr}}) = \frac{1}{2}h\|\mathbf{e}^{\text{tr}}\|^2 \quad (5)$$

with h a material parameter defining the slope of the linear linear stress - transformation strain relation in the uniaxial case.

- $\mathcal{I}_S(\mathbf{e}^{\text{tr}})$ is the indicator function of the saturation domain, i.e.:

$$\begin{cases} \mathcal{I}_S(\mathbf{e}^{\text{tr}}) = 0 & \text{if } 0 \leq \|\mathbf{e}^{\text{tr}}\| \leq \varepsilon_L \\ \mathcal{I}_S(\mathbf{e}^{\text{tr}}) = +\infty & \text{otherwise} \end{cases} \quad (6)$$

Following standard thermodynamics arguments [5], the quantities thermodynamically conjugate to the state variables are derived:

$$\begin{aligned} \boldsymbol{\sigma} &= \partial_{\mathbf{e}^e} \psi, \\ \mathbf{X} &= -\partial_{\mathbf{e}^{\text{tr}}} \psi, \\ \eta &= -\partial_T \psi. \end{aligned} \quad (7)$$

where, the symbol ∂ denotes subdifferentials in the sense of Convex Analysis, $\boldsymbol{\sigma}$ is the Cauchy stress, $\mathbf{X} \in \text{SymDev}$ is the so called transformation stress, and η is the entropy density. Equation (7)₂ is usually rewritten as:

$$\mathbf{X} = \mathbf{s} - \boldsymbol{\alpha} \quad (8)$$

where \mathbf{s} is the stress deviator, and $\boldsymbol{\alpha} \in \text{SymDev}$ is the back stress tensor, given by:

$$\boldsymbol{\alpha} = \beta\Delta T^+ \partial_{\mathbf{e}^{\text{tr}}} \|\mathbf{e}^{\text{tr}}\| + h \mathbf{e}^{\text{tr}} + \partial_{\mathbf{e}^{\text{tr}}} \mathcal{I}_S(\mathbf{e}^{\text{tr}}) \quad (9)$$

The subdifferential of the indicator function $\mathcal{I}_S(\mathbf{e}^{\text{tr}})$ results:

$$\partial_{\mathbf{e}^{\text{tr}}}\mathcal{I}_S(\mathbf{e}^{\text{tr}}) = \begin{cases} \mathbf{0} & \text{if } \|\mathbf{e}^{\text{tr}}\| < \varepsilon_L \\ \gamma \partial_{\mathbf{e}^{\text{tr}}}\|\mathbf{e}^{\text{tr}}\| & \text{if } \|\mathbf{e}^{\text{tr}}\| = \varepsilon_L \\ \emptyset & \text{if } \|\mathbf{e}^{\text{tr}}\| > \varepsilon_L \end{cases} \quad (10)$$

being $\gamma \in \mathbb{R}_0^+$ the thermodynamic reaction force associated to constraint (16), i.e.:

$$\begin{cases} \gamma = 0 & \text{if } 0 \leq \|\mathbf{e}^{\text{tr}}\| < \varepsilon_L \\ \gamma \geq 0 & \text{if } \|\mathbf{e}^{\text{tr}}\| = \varepsilon_L \end{cases} \quad (11)$$

A flow law for the transformation strain is derived assigning a *transformation function* $f(\mathbf{X})$, which defines the elastic domain in stress space $\mathcal{E} = \{\mathbf{X} \in \text{SymDev} : f(\mathbf{X}) \leq 0\}$, and invoking the postulate of maximum inelastic work [5]. It results:

$$\dot{\mathbf{e}}^{\text{tr}} = \dot{\zeta} \nabla f(\mathbf{X}) \quad (12)$$

with the Kuhn-Tucker conditions $\dot{\zeta} \geq 0$, $\dot{\zeta} f = 0$. The above results is usually referred as normality rule, and implies convexity of the elastic domain \mathcal{E} . Equivalently, the same evolution equation may be obtained introducing the dissipation pseudo-potential associated to the transformation rate $\dot{\mathbf{e}}^{\text{tr}}$:

$$D(\dot{\mathbf{e}}^{\text{tr}}) = \sup_{\mathbf{T} \in \mathcal{E}} \{\mathbf{T} : \dot{\mathbf{e}}^{\text{tr}}\} \quad (13)$$

such that $D(\dot{\mathbf{e}}^{\text{tr}}) = \mathbf{X} : \dot{\mathbf{e}}^{\text{tr}}$, being \mathbf{X} the admissible thermodynamic stress at equilibrium. Dissipation is a degree 1 positively homogeneous convex functional, null at the origin; hence, rate independence of the evolution problem follows [6].

The function $f(\mathbf{X})$ rules the activation of inelastic flow: $\dot{\mathbf{e}}^{\text{tr}} = \mathbf{0}$, if $f(\mathbf{X}) < 0$, or $\dot{\mathbf{e}}^{\text{tr}} \neq \mathbf{0}$, if $f(\mathbf{X}) = 0$. In the present context $f(\mathbf{X})$ is assumed to be deviatoric isotropic. Hence, it can be represented as $f(\rho_{\mathbf{X}}, \theta_{\mathbf{X}})$, where $\rho_{\mathbf{X}} \geq 0$, $\theta_{\mathbf{X}} \in [0, \pi/3]$ are the Haigh–Westergaard coordinates of \mathbf{X} [7, 8]. In particular, the function f is taken in the following form:

$$f(\rho_{\mathbf{X}}, \theta_{\mathbf{X}}) = \rho_{\mathbf{X}} g(\theta_{\mathbf{X}}) - \sqrt{\frac{2}{3}} \sigma_{y_0} \quad (14)$$

where g is a C^2 , positive, even, periodic function with period $2\pi/3$, such that $g'' + g > 0$; the parameter σ_{y_0} is, respectively, the initial transformation limit in tension σ_t , if $g(0) = 1$, or in compression, σ_c , if $g(\pi/3) = 1$.

2.1 Variational incremental problem

In view of implementation into a time marching solution procedure, the rate equations reported in the previous section are integrated in time, applying the backward Euler

integration scheme. Reference is made to time instants t_n , and $t_{n+1} > t_n$, with time step $\Delta t := t_{n+1} - t_n$ and to the corresponding increment of state variables $(\Delta \boldsymbol{\varepsilon}, \Delta \mathbf{e}^{\text{tr}}, \Delta T)$. The material state and the stress are known at t_n and the increment of strain and temperature $\Delta \boldsymbol{\varepsilon}$, and ΔT are given, leading to the values $\boldsymbol{\varepsilon}_{n+1} = \boldsymbol{\varepsilon}_n + \Delta \boldsymbol{\varepsilon}$, and $T_{n+1} = T_n + \Delta T$, at t_{n+1} .

Recongnizing $\Delta \mathbf{e}^{\text{tr}}$ as the main unknown, the material state evolution obeys to the following variational problem in incremental form [9]:

$$\mathcal{F}^{\text{incr}} = \inf_{\substack{\{\Delta \mathbf{e}^{\text{tr}}\} \\ c(\Delta \mathbf{e}^{\text{tr}}) \leq 0}} \left\{ \psi(\boldsymbol{\varepsilon}_{n+1} - \mathbf{e}_n^{\text{tr}} - \Delta \mathbf{e}^{\text{tr}}, \mathbf{e}_n^{\text{tr}} + \Delta \mathbf{e}^{\text{tr}}, T_{n+1}) + D(\Delta \mathbf{e}^{\text{tr}}) \right\}. \quad (15)$$

where $c(\Delta \mathbf{e}^{\text{tr}})$ represents the unilateral saturation constraint, i.e.:

$$c(\Delta \mathbf{e}^{\text{tr}}) = \frac{\|\mathbf{e}_n^{\text{tr}} + \Delta \mathbf{e}^{\text{tr}}\|^2}{\varepsilon_L^2} - 1 \quad (16)$$

Introducing the Lagrangian associated to variational problem (15):

$$\mathcal{L}(\Delta \mathbf{e}^{\text{tr}}, \gamma) = \psi(\boldsymbol{\varepsilon}_{n+1} - \mathbf{e}_n^{\text{tr}} - \Delta \mathbf{e}^{\text{tr}}, \mathbf{e}_n^{\text{tr}} + \Delta \mathbf{e}^{\text{tr}}, T_{n+1}) + D(\Delta \mathbf{e}^{\text{tr}}) + \gamma c(\Delta \mathbf{e}^{\text{tr}}), \quad (17)$$

with γ a Kuhn-Tucker multiplier for $c(\Delta \mathbf{e}^{\text{tr}})$, stationary conditions for problem (17) are:

$$\begin{aligned} -\partial_{\Delta \mathbf{e}^{\text{tr}}} \psi(\boldsymbol{\varepsilon}_{n+1} - \mathbf{e}_n^{\text{tr}} - \Delta \mathbf{e}^{\text{tr}}, \mathbf{e}_n^{\text{tr}} + \Delta \mathbf{e}^{\text{tr}}, T_{n+1}) - \gamma \partial c(\Delta \mathbf{e}^{\text{tr}}) &\in \partial D(\Delta \mathbf{e}^{\text{tr}}), \\ c(\Delta \mathbf{e}^{\text{tr}}) &\leq 0, \end{aligned} \quad (18)$$

with the complementary conditions: $\gamma \geq 0$, $c\gamma = 0$.

3 SOLUTION ALGORITHM

The evolution of the material state for the SMA constitutive model under investigation is governed by the constrained nonlinear differential inclusion eq. (18). The residual form of those equations is:

$$\mathbf{r}(\mathbf{x}) := \begin{cases} -\mathbf{X}_{n+1}(\boldsymbol{\varepsilon}_{n+1}, \Delta \mathbf{e}^{\text{tr}}, T_{n+1}) + \partial D(\Delta \mathbf{e}^{\text{tr}}) + \gamma \partial c(\Delta \mathbf{e}^{\text{tr}}) \\ c(\Delta \mathbf{e}^{\text{tr}}) \end{cases} \quad \text{for } \mathbf{x} := \begin{cases} \Delta \mathbf{e}^{\text{tr}} \\ \gamma \end{cases} \quad (19)$$

being:

$$\begin{aligned} \mathbf{X}_{n+1}(\boldsymbol{\varepsilon}_{n+1}, \Delta \mathbf{e}^{\text{tr}}, T_{n+1}) &:= -\partial_{\Delta \mathbf{e}^{\text{tr}}} (\psi^e(\boldsymbol{\varepsilon}_{n+1} - \mathbf{e}_n^{\text{tr}} - \Delta \mathbf{e}^{\text{tr}}) + \psi^{\text{ch}}(\mathbf{e}_n^{\text{tr}} + \Delta \mathbf{e}^{\text{tr}}, T_{n+1}) + \\ &\quad + \psi^{\text{tr}}(\mathbf{e}_n^{\text{tr}} + \Delta \mathbf{e}^{\text{tr}})) \end{aligned} \quad (20)$$

Eq. (19) is solved with Newton-Raphson method, using the consistent tangent:

$$\mathbb{T} = \begin{bmatrix} \mathcal{H}_{\Delta \mathbf{e}^{\text{tr}}} \psi(\boldsymbol{\varepsilon}_{n+1}, \Delta \mathbf{e}^{\text{tr}}, T_{n+1}) + \mathcal{H}D(\Delta \mathbf{e}^{\text{tr}}) & \nabla c(\Delta \mathbf{e}^{\text{tr}}) \\ \nabla^t c(\Delta \mathbf{e}^{\text{tr}}) & 0 \end{bmatrix} \quad (21)$$

The Hessian $\mathcal{H}_{\Delta \mathbf{e}^{\text{tr}} \psi}(\boldsymbol{\varepsilon}_{n+1}, \Delta \mathbf{e}^{\text{tr}}, T_{n+1})$ and $\mathcal{H}D(\Delta \mathbf{e}^{\text{tr}})$ may be found explicitly in [10].

Solution of the equations (19) presents numerical difficulties since each of the sub-gradients $\partial \psi^{\text{ch}}(\mathbf{e}_{n+1}^{\text{tr}})$ and $\partial D(\Delta \mathbf{e}^{\text{tr}})$, becomes a set if the solution coincides with their respective singularity point: $\mathbf{e}_{n+1}^{\text{tr}} = \mathbf{0}$ (i.e. $\Delta \mathbf{e}^{\text{tr}} = -\mathbf{e}_n^{\text{tr}}$), and $\Delta \mathbf{e}^{\text{tr}} = \mathbf{0}$: In any of those cases:

$$\partial \psi^{\text{ch}}(\mathbf{0}, T_{n+1}) = \{ \mathbf{T} \in \text{SymDev} : \|\mathbf{T}\| \leq \beta \Delta T^+ \} \quad (22)$$

$$\partial D(\mathbf{0}) = \{ \mathbf{T} \in \text{SymDev} : f(\mathbf{T}) \leq 0 \} \equiv \mathcal{E} \quad (23)$$

and the corresponding Hessians are unbounded. In order to have a robust solution scheme, the proposed solution algorithm proceeds as follows:

1. Check if solution coincides with any singularity point;
2. If check 1. is not satisfied, then solve (19) for a regular solution, expectedly far from any singularity point, via Newton-Raphson method;
3. If solution 2. is not found, then check if solution is neighboring any singularity point.

3.1 Check on singularity point solutions

Admissibility of a singularity point solution requires to verify if such particular solution satisfies eq. (18). To this end, the *trial* transformation stress $\mathbf{X}_{n+1}^{\text{trial}}(\boldsymbol{\varepsilon}_{n+1}, \Delta \mathbf{e}^{\text{tr}}, T_{n+1})$, relative to the regular part of the free energy ψ^{reg} , is introduced. Four cases may be distinguished:

(S.1) $\Delta \mathbf{e}^{\text{tr}} = \mathbf{0}$, $\|\mathbf{e}_{n+1}^{\text{tr}}\| < \varepsilon_L$. In this case: $\psi^{\text{reg}} = \psi^e + \psi^{\text{tr}} + \psi^{\text{ch}}$.

Setting $\mathbf{X}_{n+1}^{\text{trial}} = -\nabla \psi^{\text{reg}}|_{\Delta \mathbf{e}^{\text{tr}}=\mathbf{0}}$, the thermodynamic inclusion becomes:

$$\mathbf{X}_{n+1}^{\text{trial}} \in \mathcal{E}, \quad (24)$$

to be verified by checking if $f(\mathbf{X}_{n+1}^{\text{trial}}) \leq 0$.

(S.2) $\Delta \mathbf{e}^{\text{tr}} = \mathbf{0}$, $\|\mathbf{e}_{n+1}^{\text{tr}}\| = \varepsilon_L$. In this case: $\psi^{\text{reg}} = \psi^e + \psi^{\text{tr}} + \psi^{\text{ch}}$.

Setting $\mathbf{X}_{n+1}^{\text{trial}} = -\nabla \psi^{\text{reg}}|_{\Delta \mathbf{e}^{\text{tr}}=\mathbf{0}}$, the thermodynamic inclusion becomes:

$$\mathbf{X}_{n+1}^{\text{trial}} - \gamma \nabla c(\mathbf{0}) \in \mathcal{E}, \quad (25)$$

to be verified by checking if there exists $\gamma > 0$, such that $f(\mathbf{X}_{n+1}^{\text{trial}} - \gamma \nabla c(\mathbf{0})) = 0$, i.e. by searching a zero of a convex scalar function.

(S.3) $\mathbf{e}_{n+1}^{\text{tr}} = \mathbf{0}$. In this case: $\psi^{\text{reg}} = \psi^e + \psi^{\text{tr}}$.

Setting $\mathbf{X}_{n+1}^{\text{trial}} = -\nabla \psi^{\text{reg}}|_{\Delta \mathbf{e}^{\text{tr}}=-\mathbf{e}_n^{\text{tr}}}$, the thermodynamic inclusion becomes:

$$\mathbf{X}_{n+1}^{\text{trial}} - \nabla D(-\mathbf{e}_n^{\text{tr}}) \in \partial \psi^{\text{ch}}(\mathbf{0}), \quad (26)$$

to be verified by checking if $\|\mathbf{X}_{n+1}^{\text{trial}} - \nabla D(-\mathbf{e}_n^{\text{tr}})\| \leq \beta \Delta T^+$.

Table 1: SMA material properties.

E	h	ν	ε_L	M_f	β	σ_{y_0}
70000 MPa	500 MPa	0.33	0.03	253.15 K	7.5 MPa K ⁻¹	45 MPa

(S.4) $\Delta \mathbf{e}^{\text{tr}} = \mathbf{0}$, $\mathbf{e}_{n+1}^{\text{tr}} = \mathbf{0}$. In this case: $\psi^{\text{reg}} = \psi^e + \psi^{\text{tr}}$.

Setting $\mathbf{X}_{n+1}^{\text{trial}} = -\nabla \psi^{\text{reg}}|_{\Delta \mathbf{e}^{\text{tr}} = \mathbf{e}_{n+1}^{\text{tr}} = \mathbf{0}}$, with $\psi^{\text{reg}} = \psi^e + \psi^{\text{tr}}$, the thermodynamic inclusion becomes:

$$\mathbf{X}_{n+1}^{\text{trial}} \in \nabla D(\mathbf{0}) + \partial \psi^{\text{ch}}(\mathbf{0}), \quad (27)$$

to be verified by checking if $\mathbf{X}_{n+1}^{\text{proj}}$, the orthogonal projection of $\mathbf{X}_{n+1}^{\text{trial}}$ onto $\nabla D(\mathbf{0}) \equiv \mathcal{E}$, satisfies the inequality $\|\mathbf{X}_{n+1}^{\text{trial}} - \mathbf{X}_{n+1}^{\text{proj}}\| \leq \beta \Delta T^+$. The sketch of step 3., with the checks on nearly singular cases, is omitted here, for brevity reasons. Details can be found in reference [10].

4 NUMERICAL TESTS

The efficiency of the proposed state update algorithm in checking and treating the singular and nearly singular cases previously examined, is demonstrated by solving some selected isothermal non-proportional biaxial loading histories, under mixed stress-strain control [4]. In particular, an initial boundary value problem is considered, by prescribing two strain components and keeping equal to zero the stress components corresponding to the non-controlled strains. A two-level solution is applied: a Newton method is used to solve the equation enforcing zero stress components; at a lower level, the state update algorithm solves the constitutive equations for the transformation strain, computes the stress tensor plus the consistent material tangent stiffness, required by the upper level solver to advance iteratively. This test setup tackles specifically the question of accuracy and robustness of the state update algorithm and of accuracy of the material tangent stiffness operator.

Material properties [4] for the present numerical simulations are reported in Table 1, assuming the material in the parent phase (i.e. $\|\mathbf{e}^{\text{tr}}\| = 0$) at the beginning of a loading history. For simplicity, the prescribed stress tensor $\bar{\boldsymbol{\sigma}}$ has a piece-wise linear evolution in time starting from zero. A von Mises transformation function is chosen, i.e. $g(\theta_{\mathbf{x}}) = 1$.

4.1 Non-proportional biaxial hourglass loading histories

The test is carried out at constant temperature $T = 285.15$ K. The controlled strain components vary according to the time history reported in Tab. 2, where they are indicated generically as $\bar{\boldsymbol{\varepsilon}}_1$ and $\bar{\boldsymbol{\varepsilon}}_2$, respectively. Two loading histories are examined. The first one sets $\bar{\boldsymbol{\varepsilon}}_1 = \varepsilon_{11}$, $\bar{\boldsymbol{\varepsilon}}_2 = \varepsilon_{22}$, the second one sets $\bar{\boldsymbol{\varepsilon}}_1 = \varepsilon_{11}$, $\bar{\boldsymbol{\varepsilon}}_2 = \gamma_{12}$.

Figures 1 and 2, respectively, report the material response in terms the stress compo-

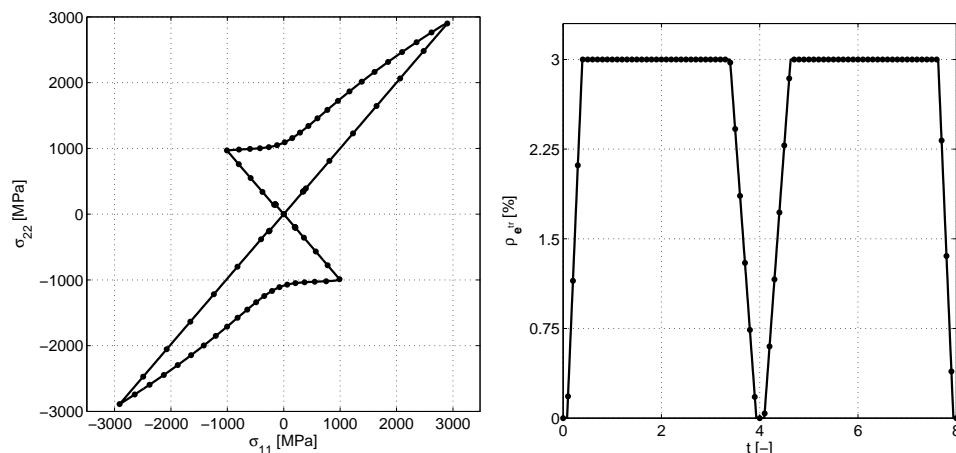


Figure 1: Non-proportional biaxial hourglass test for controlled strain components $\varepsilon_{11} - \varepsilon_{22}$. $T = 285.15$ K. Stress plot σ_{22} vs. σ_{11} (L). Transformation strain norm plot $\rho_{e^{tr}}$ vs. time t (R). Fine time discretization: $\Delta t = 1/100$ (continuous line); coarse time discretization: $\Delta t = 1/10$ (bullets).

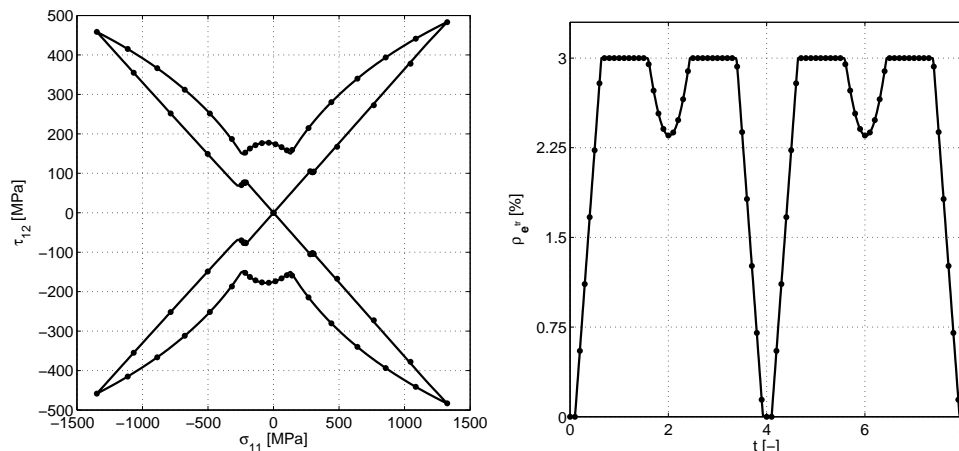


Figure 2: Non-proportional biaxial hourglass test for controlled strain components $\varepsilon_{11} - \gamma_{12}$. $T = 285.15$ K. Stress plot τ_{12} vs. σ_{11} (L). Transformation strain norm plot $\rho_{e^{tr}}$ vs. time t (R). Fine time discretization: $\Delta t = 1/100$ (continuous line); coarse time discretization: $\Delta t = 1/10$ (bullets).

Table 2: Non-proportional biaxial hourglass loading history. Time history for controlled strain components. $\bar{\varepsilon}^{\max} = 4\%$

t	0	1	2	3	4	5	6	7	8
$\bar{\varepsilon}_1$	0	$\bar{\varepsilon}^{\max}$	0	$-\bar{\varepsilon}^{\max}$	0	$\bar{\varepsilon}^{\max}$	0	$-\bar{\varepsilon}^{\max}$	0
$\bar{\varepsilon}_2$	0	$\bar{\varepsilon}^{\max}$	$\bar{\varepsilon}^{\max}$	$\bar{\varepsilon}^{\max}$	0	$-\bar{\varepsilon}^{\max}$	$-\bar{\varepsilon}^{\max}$	$-\bar{\varepsilon}^{\max}$	0

nents dual of the controlled strains, highlighting the strongly nonlinear character of the constitutive behavior for non-proportional loading. Each loading history is solved adopting a coarse and a fine time discretization: no sensitivity to time discretization is observed. Furthermore, the plots of transformation strain norm $\rho_{\mathbf{e}^{\text{tr}}}$ vs time enlighten the algorithm capability to check and treat the singularity points solution as well as nearly-singular solutions. Noteworthy, the quantity $\rho_{\mathbf{e}^{\text{tr}}}$ computed with the proposed method presents the expected sharp threshold at the beginning of the phase transition; such would not be the case applying a transformation strain norm regularization, to overcome the singularity $\mathbf{e}^{\text{tr}} = \mathbf{0}$ [3].

5 CONCLUSIONS

In this paper an innovative dissipation-based solution algorithm for 3D phenomenological constitutive models for SMA has been presented. The key features of the proposed methodology are: (i) the detection and treatment of singularities inherent to the energy formulation of the constitutive model, without any regularization of the constitutive equations; (ii) an efficient computation of the dissipation function and its derivatives, adopting the Haigh-Westergaard invariants of the transformation stress; (iii) an extension on the choice of the transformation function and hence on the activation criterion for phase transition; iv a robust constitutive solver for finite element simulation.

REFERENCES

- [1] B.D. Coleman and M.E. Gurtin. Error estimates for discretizations of a rate-independent variational inequality. *J. Chem. Phys.* (1967) **47**:597–613.
- [2] Souza A, Mamiya E, Zouain N. Three-dimensional model for solids undergoing stress-induced phase transformations. *Eur. J. Mech., A- Solid* (1998) **17**:789–806.
- [3] Auricchio F, Petrini L. A three-dimensional model describing stress-temperature induced solid phase transformations: solution algorithm and boundary value problems. *Int. J. Numer. Meth. Eng.* (2004) **61**:807–836.
- [4] Auricchio F, Petrini L. Improvements and algorithmical considerations on a recent three-dimensional model describing stress-induced solid phase transformations. *Int. J. Numer. Meth. Eng.* (2002) **55**:1255–1284.
- [5] Han W, Reddy BD. *Plasticity: Mathematical Theory and Numerical Analysis*. Springer-Verlag: New York, (1999).
- [6] Auricchio F, Mielke A, Stefanelli U. A rate-independent model for the isothermal quasi-static evolution of shape-memory materials. *Math. Mod. Meth. Appl. S.* (2008) **18**:125–164.

- [7] Lode W. Versuche über den Einfluss der mittleren Hauptspannung auf das Fließen der Metalle Eisen Kupfer und Nickel. *Zeitung Phys.* (1926) **36**:913–939.
- [8] Nayak GC, Zienkiewicz OC. Convenient forms of stress invariants for plasticity. *Proceedings of the ASCE Journal of the Structural Division* (1972) **98**(ST4):949–953.
- [9] Hackl K, Fischer F. On the relation between the principle of maximum dissipation and inelastic evolution given by dissipation potentials. *P. Roy. Soc. A-Math. Phy.* (2008) **464**:1172–132.
- [10] Artioli E, Bisegna P. A dissipation-based solution algorithm for 3D phenomenological SMA constitutive models. *Int. J. Numer. Meth. Eng.* (2014) submitted.